LDRNet: Enabling Real-time Document Localization on Mobile Devices

Han Wu*

Newcastle University

United Kingdom

han.wu@ncl.ack.uk

Holland Qian*

Tencent
China
niuwa.frog@gmail.com

Huaming Wu
Tianjin University
China
whming@tju.edu.cn

Abstract—While Identity Document Verification (IDV) technology on mobile devices becomes ubiquitous in modern business operations, the risk of identity theft and fraud is increasing. The identity document holder is normally required to participate in an online video interview to circumvent impostors. However, the current IDV process depends on an additional human workforce to support online step-by-step guidance which is inefficient and expensive. The performance of existing AI-based approaches cannot meet the real-time and lightweight demands of mobile devices. In this paper, we address those challenges by designing an edge intelligence-assisted approach for real-time IDV. Aiming at improving the responsiveness of the IDV process, we propose a new document localization model for mobile devices, LDRNet, to Localize the identity Document in Real-time. On the basis of a lightweight backbone network, we build three prediction branches for LDRNet, the corner points prediction, the line borders prediction and the document classification. We design novel supplementary targets, the equal-division points, and use a new loss function named Line Loss, to improve the speed and accuracy of our approach. In addition to the IDV process, LDRNet is an efficient and reliable document localization alternative for all kinds of mobile applications. As a matter of proof, we compare the performance of LDRNet with other popular approaches on localizing general document datasets. The experimental results show that LDRNet runs at a speed up to 790 FPS which is 47x faster, while still achieving comparable Jaccard Index(JI) in single-model and single-scale tests.

Index Terms—Document localization, Identity Verification, Edge Intelligence, Mobile Devices.

I. INTRODUCTION

The outbreak of COVID-19 brings a detrimental impact on human health and the global economy with a ripple effect on every aspect of civic life [1]. One indubitable fact is that the lockdowns and quarantine policies accelerate the economic community to shift most business operations to online mode. The Identity Document Verification (IDV) technology is increasingly adopted by financial service organizations as a direct consequence of the pandemic. IDV aims to verify the authenticity of user identity through the photos or videos containing their identity documents. However, these visual materials are generally captured by smartphones thus can be easily exploited by fraudsters and impostors.

Basically, the IDV process consists of two parts. The first is verifying whether the provided identity document is authentic. The other process is checking if the person who

provides the document is linked with the presented identity document, which is under high risk when the entire process runs online. For instance, in the case of data leakage, the exposed image of the victim's identity document may be exploited by impostors. The existing solution is by doing an online interview, where the user presents the identity document in the video chat with the verifier's human service. This approach has become a strategic imperative for businesses to establish trust with customers online. However, it requires an additional human workforce as guidance, while existing artificial intelligence(AI)-based solutions are not applicable on mobile devices.

To this end, we propose an edge intelligence-assisted approach to take the place of the above online interview process. The link between the user and the presented identity document is verified based on biometric traits captured by the smartphone camera. By recording a video in the mobile application, the user is required to move the identity document correctly following the step-by-step instructions. In our design the edge intelligence technology is expected to detect the identity document in this live video and make movement judgments in real-time. This is also the main research challenge that needs to be addressed beforehand. Running current deep learning models on mobile devices is very resource-intensive and requires highend processors to be equipped [2]. The reason behind this is their low efficiency of localizing documents captured in a live video.

Generally, document localization [3] is a technology that focuses on detecting and segmenting document outlines within image frames. The inputs are usually a set of digital photos (i.e. the frames of a video) containing the document. The outputs are the quadrilateral coordinates of document outlines per frame. The identity document in the case of IDV is expected to be localized in real-time since image frames in a live video are generated at high frequency and the quick response from the guidance module is imperative for smooth interaction. However, existing document localization approaches can not fulfill these real-time demands due to the long inference time. Furthermore, the state-of-the-art document localization models are complex and require large storage space, which exhausts the capacity of smartphones.

To break through this bottleneck we propose a novel document localization network, LDRNet, to Localize Document

^{*}Equal contribution

in Real-time. Previous works dive into the design of the new network architectures to improve the accuracy, which is time-consuming and diminishes the efficiency. We start from a lightweight Convolutional Neural Network (CNN), MobilenetV2 [4], which is a fundamental feature extractor especially designed for devices with limited memory and resources [5]. Unlike feature pyramid networks [6], we design a feature fusion module that does not enlarge the model size. Existing document localization approaches require postprocessing after prediction, which is cumbersome and inefficient. Therefore we design our prediction target to be the coordinates of the quadrilateral corners instead of the contour of the document thus avoiding postprocessing. The orientation of the document also can be obtained from the order of the output coordinates. For guaranteeing precision, we propose a novel loss function, Line Loss, as a new metric for document localization. By adding equal-division points between contiguous corner points, LDRNet achieves better formalization of the borderlines.

In summary, the main contributions of this paper include:

- We present LDRNet, a document localization approach with significantly lower computational cost than the stateof-the-art methods. LDRNet paves the way for our edge intelligence-assisted IDV framework. We apply this IDV framework in real business and it has supported over 50,000 customers to open their bank accounts.
- We design the Line Loss function and equal-division points feature for LDRNet to guarantee the localization accuracy without undermining its efficiency or enlarging its model size. The average Jaccard Index (JI) of LDRNet achieves 0.9849 to the highest in our experiment, which is comparable with other state-of-the-art models.
- Moreover, the role of LDRNet goes far beyond identity document localization. In the experiments, we compare the performance of LDRNet with other popular approaches on localizing general document datasets. The results indicate that LDRNet is a reliable approach to localize any type of document in real-time.

II. RELATED WORK

There exist three main kinds of approaches for document localization, namely, *Mathematical Morphology-based Methods*, *Segmentation-based Methods* and *Keypoint-like Methods*. Mathematical morphology-based methods are based on mathematical morphology [7]. Many methods [8], [9] use geometric analysis to find edges first by adopting Canny edge detector or Line Segment Detector (LSD) [10], etc. There are some other hand-designed features used in mathematical morphology-based methods, like the tree-based representation [11] and the connected operators filtering [12]. Along with the popularity of CNN in this field, many CNN-based methods have emerged. Segmentation-based methods regard document localization as the segmentation [13] task using the CNN to extract the features. Same as segmentation-based methods, using the features extracted by the CNN, keypoint-like methods [14] predict the

four corners of the document directly, considering document localization as the keypoint detection task [15].

Mathematical Morphology-based Methods inherit the ideas which detect the contour of the documents using traditional image processing methods, image gradients calculations [16], Canny edge detectors, Line Segment detectors [10] and image contours detectors, etc. Although there are many kinds of different mathematical morphology-based approaches, they are all developed on the basis of the technologies mentioned above, which makes the performance unstable when the datasets change. The accuracy of these methods heavily depends on the environmental conditions in the image. For instance, if the color of the background and the document are difficult to distinguish, or if the image is captured with insufficient lighting, the edges of the document may not be detected. Another weakness of these mathematical morphology-based methods is that they output the four edges or four points disorderly so a necessary step for determining the orientation of the document is the postprocessing, which leads to extra cost.

Segmentation-based Methods regard document localization as a segmentation task. Segmentation adapts dense predictions, outputs the heat map for every pixel on the image, and uses classification labels to determine whether the pixels belong to the object or the background. Then by grouping the pixels with the same labels, the document is segmented. By adopting the CNNs to extract the image feature, the segmentors get rid of the impacts from the complex environment conditions. Since every segmentor is a data-driven deep-learning model, it can reach high precision as long as enough data are fed. U-Net [6], DeepLab [17] and FCN [18] are all popular segmentors. However, the large model size and high model latency make these segmentors incompetent for real-time document localization. Similar to the mathematical morphology-based methods, postprocessing is inevitable to find the orientation of the document content.

Keypoint-like Methods output the coordinates of the quadrilateral corner points of the document directly. Recent keypoint detection networks do not regress the coordinates of the key points, instead, they produce dense predictions like segmentation networks do. [19] predict heat maps of the keypoints and offsets. [20] achieve state-of-the-art results on the MPII and LSP datasets by producing heat maps. [14] predict the points in a sparse-prediction way to locate the four points directly. To improve the precision, it uses CNN recursively to fix the coordinates errors. These keypoint models indeed get high precision, but also have the same weakness which segmentation-based methods have, the large model size and the high model latency.

III. OUR APPROACH

Edge Intelligence is generally described as the paradigm of running AI algorithms locally on an end device, where the data are generated [2]. Our edge intelligence-assisted approach is a device-based model, which means the mobile device holds the document localization model and performs model inference locally. The mobile device does not need to communicate with the cloud server during the inference process. In this section, we firstly introduce the proposed edge intelligence-assisted IDV framework and explain why real-time identity document localization is critical in the center. Then we present our comprehension of the document localization task, and reformulate document localization in a single regression fashion. Next, we introduce the novel points in our network architecture, including equal-division points and Line Loss.

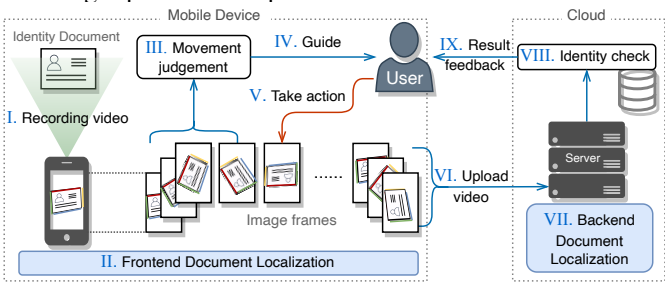


Fig. 1: Overview of the edge intelligence-assisted identity document verification workflow.

A. Edge Intelligence-assisted IDV System Design

Our Edge Intelligence-assisted Identity Document Verification (IDV) system consists of two parts: (i) on the frontend (i.e. mobile devices), the IDV application guides the user to take a video of the identity document. (ii) on the backend (i.e. servers), the uploaded video is analyzed by IDV system to generate verification results. As the workflow depicted in Fig. 1, when the user continues to record the video (step I), each image frame is processed by LDRNet to localize the identity document (step II). According to a series of previous localization results, the IDV application judges the document's movement performed by the user (step III) and sends the action guidance including a sequence of the specific speed and directions to the user (step IV). The user follows these instructions to rotate, move or flip over the document (step V) until the video is recorded and uploaded to the backend (step VI). LDRNet is also applied on the backend to localize identity documents in the uploaded video (step VII), facilitating the IDV system to extract necessary information. After checking the extracted identity information (step VIII), the system returns the identity verification result to the user (step IX).

1) Components of the IDV System: Frontend: The IDV frontend aims at capturing the identity document as well as the user's biometric traits in a video and uploading it to the backend. Instead of separated photos, a continuous video contains complete behavioral biometrics of the user, which is essential for detecting impostors. Furthermore, the identity document normally contains laser security marks for anticounterfeiting. The color and shape of these marks change dynamically depending on the light environment and camera angle. The recorded video captures all these dynamics thus providing more comprehensive materials for the verification process. To successfully record the video, the user is required to perform a series of operations on the identity document following the step-by-step guidance in the frontend. An example of this interaction is shown in Fig. 2, where the frontend application instructs the user to turn the identity document slowly to the left. Once the user's operation is approved, the next guidance is displayed on the screen and the user needs to repeat this several times (e.g. four times in our business) until the recording finishes.







(1) guidance displayed (2) user performs action

(3) action approved

Fig. 2: An example of the interaction on the IDV frontend.

To ensure a smooth user experience and provide reliable materials for the backend, the frontend application should detect the trajectory of the identity document and respond to the user in real-time. This calls for strict demands on both the accuracy and speed of document localization, which are the bottleneck of implementing the proposed IDV system. Specifically, the challenges come from four facets: (i) In addition to the contour of the identity document, the direction of the content should also be detected to determine the trajectory of the document. (ii) It is complex and time-consuming to calculate the precise angle between the identity document and the camera to obtain the trajectory. (iii) The corner points of the document may be occluded by the user's fingers, therefore the ability to predict occluded corner points is necessary. (iv) While the video is being recorded, images are generated at high frequency (e.g. 30 FPS) but the computational resource on a smartphone is very limited. Additionally, the responsiveness of the IDV application is critical as the user needs to perform corrective action guided by the application in real-time.

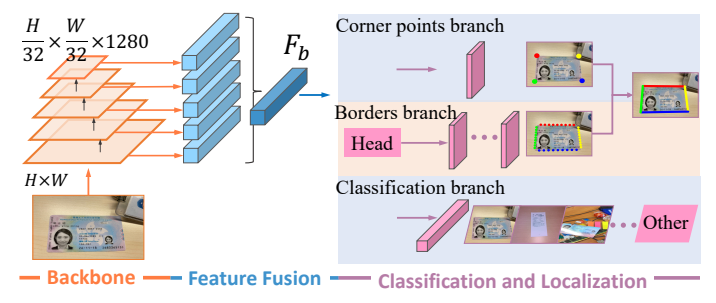


Fig. 3: The network architecture of LDRNet.

2) Components of the IDV System: Backend: Once the video has been successfully uploaded to the server, the backend extracts all the information required for identity verification. Precise document localization of each image frame is the prerequisite for all subsequent processes. On the backend, our document localization approach is designed to be accuracyprioritized because there are plentiful computational resources. Then the backend performs a perspective transformation on the localized document on each image frame. The warped frames are sent to the classification module to obtain the category of the identity document. Popular classification approaches include C3D [21] and CNN+LSTM [22]. Finally, the verification result is generated and sent back to the frontend. Since the research challenge on the backend is minor, we will not dive into the details in this paper.

B. Task Analysis

To address the challenges listed above, we present a novel neural network model, LDRNet, to Localize Documents in Real-time. Instead of calculating the precise angle between the document and camera, we calculate the distance between each target corner point and the corresponding localized point to track the trajectory of the document. This provides considerable accuracy while consuming less computational resources on smartphones. As summarized by the following equation, (x^i_{doc}, y^i_{doc}) is the coordinate of the ith corner point of the localized document, while $(x^i_{target}, y^i_{target})$ represents the coordinate of the ith target corner point. Then we sum the Euclidean distances of the four sets of corresponding points.

$$Distance = \sum_{i=1}^{4} \left[(x_{doc}^{i} - x_{target}^{i})^{2} + (y_{doc}^{i} - y_{target}^{i})^{2} \right].$$
 (1)

The orientation of the document can be simply inferred from the order of the corner points. Thus our goal is to predict the four quadrilateral coordinates of the document, which are named left top corner point (LT), left bottom corner point(LB), right bottom corner point (RB) and right top corner point (RT) in counter-clockwise order, respectively. The order of the four quadrilateral points is determined by the contents of the document instead of the direction that the document is placed. In the remainder of this paper, we use the red point to denote LT, green for the LB, blue for the RB and yellow for RT. In our model, we predict N points in total. In addition to the four corner points, we predict (N-4)/4 equal-division points on each edge of the document. These extra N-4 points are used to refine the localization of the document. Moreover, we add a classification head to our network architecture for classifying the document in the input images. For instance, it can classify the passports depending on the nationality. The minimum number of classes is two, which represents whether the image contains a document or not, respectively.

C. Network Architecture

1) Fully Convolutional Feature Extractor: As we aim to run document localization on mobile devices, we choose a lightweight backbone network, MobilenetV2 [4]. It applies both depth-wise convolution and point-wise convolution operations to achieve faster and lighter extraction. As illustrated in Fig. 3, the last output feature map from the backbone is $F_b \in R^{\frac{H}{32}*\frac{W}{32}*1280}$ with H denoting the height of the input image and W denoting the width. To improve the accuracy,

we extract five feature maps with different spatial resolutions from the backbone.

- 2) Feature Fusion Module: The low and high-level feature maps are fused together by the feature fusion module. The first step is feature compression, where we use global average pooling to downsample the feature maps, and resize them to the same size. Then we add the five feature maps directly instead of the top-down architecture used in [23]. Our method avoids introducing numerous parameters and simplifies the calculation steps. More details of how we construct this module are described in Section IV-E.
- 3) Network Output Branches: The outputs of the LDRNet consist of three branches. The first branch is the corner points branch. It outputs in the form of a 4*2 vector, four corners' coordinates (x,y) in order. The second branch is the borders branch, it outputs in the form of an (N-4)*2 vector, where (N-4) is the number of points to be predicted on the four borders. Each border has (N-4)/4 points so there are N-4 coordinates of points in total on the second branch. The third branch outputs the classification label, denoting the type of document in the input image. Unless the size of the classification output is specified, the classification output contains two elements, one denoting the likelihood of having documents in the image, the other one denoting the likelihood that no document is detected in the input image.
- 4) Line Loss: Standard Deep Convolutional Neural Network architectures are inherently poor at precise localization and segmentation tasks [24]. This is because the last convolutional layer only contains high-level features of the whole image. While these features are extremely useful for classification and bounding box detection, they lack the information for pixel-level segmentation [14]. In order to improve the precision of document localization, we combine the two branches of the LDRNet's outputs (corner points branch and borders branch), we predict the corners in a line-prediction fashion. In addition to the four corner points, we also predict the equal-division points on the lines thus the labels can be generated automatically and no more human effort is required. The proposed **Line Loss** is defined as a weighted sum of the similarity loss L_{Sim} and the distance loss L_{Dis} , which can be formulated as:

$$L_{line}(p) = \beta L_{Sim}(p) + \gamma L_{Dis}(p), \tag{2}$$

where β and γ are weighting parameters. The similarity loss is used to restrict the points from the same edge along an identical line, while the distance loss is used to guarantee that along this line the points are equally divided as shown in Fig. 4. Only the Line Loss on the right edge is illustrated in Fig. 4 (c). During the training process, we calculate the losses on all the fours edges.

To guarantee that the predicted points from each edge are on a straight line, we use the **similarity loss** L_{Sim} to calculate the similarity of two vectors of the three successive points as shown in Fig. 4. The details of L_{Sim} are shown in Eq. (3),



Text



(a) Predicting 4 points

(b) Predicting 16 points

(c) Predicting 16 points with Line Loss

Fig. 4: Improvement of the 16 points prediction, with and without the Line Loss.

(4), (5).

$$L_{Sim}(p) = \frac{\sum_{k \in l, r, t, b} \sum_{i=0}^{\frac{N}{4} - 1} sim(p[k]_i, p[k]_{i+1}, p[k]_{i+2})}{N - 4}.$$

(3)

$$sim(p[k]_i, p[k]_{i+1}, p[k]_{i+2}) = \frac{\overrightarrow{p[k]_i^{i+1}} \cdot \overrightarrow{p[k]_{i+1}^{i+2}}}{\left|\overrightarrow{p[k]_i^{i+1}}\right| \times \left|\overrightarrow{p[k]_{i+1}^{i+2}}\right|}, \tag{4}$$

$$\overrightarrow{p[k]_{i}^{i+1}} = \left(p[k]_{i}^{x} - p[k]_{i+1}^{x}, p[k]_{i}^{y} - p[k]_{i+1}^{y}\right). \tag{5}$$

where p[l], p[r], p[t], p[b] denote the points on the left edge, on the right edge, on the top edge and on the bottom edge, respectively.

The **distance loss** is used to constrain the points we predict to be equal-division points. We use Eqs. (6) and (7) to make sure the successive points of each edge have the same distance in both x-direction and y-direction.

$$L_{Dis}(p) = \frac{\sum_{k \in l, r, t, d} \sum_{i=0}^{\frac{N}{4} - 1} dist(p[k]_i, p[k]_{i+1}, p[k]_{i+2})}{N - 4},$$
(6)

$$dist(p[k]_{i}, p[k]_{i+1}, p[k]_{i+2}) = ||p[k]_{i}^{x} - p[k]_{i+1}^{x}| - |p[k]_{i+1}^{x} - p[k]_{i+2}^{x}|| + ||p[k]_{i}^{y} - p[k]_{i+1}^{y}| - |p[k]_{i+1}^{y} - p[k]_{i+2}^{y}||.$$
(7)

Furthermore, we use L2 loss for the regression and cross-entropy for the classification. The **regression loss** L_{Reg} is an L2 loss between the predicted points p and the ground truth points q, which can be formulated as:

$$L_{Reg}(p,g) = \frac{1}{N-4} \sum_{i=0}^{N} \sum_{j \in x,y} \sqrt[2]{(\hat{g}_i^j - p_i^j)^2}, \quad (8)$$

$$\hat{g}^x = g^x / W, \tag{9}$$

$$\hat{g}^y = g^y / H. \tag{10}$$

where (g_i^x, g_i^y) denotes the *i*-th ground truth point of the document. Our regression target is \hat{g} , which is the normalization of g by image width (W) in x-coordinate and image height (H) in y-coordinate. N is the number of points we predict for each document.

The **classification loss** L_{Cls} is soft-max loss over multiple classes confidences (x), which is calculated as:

$$L_{Cls}(x,c) = \sum_{i=0}^{N_{cls}} -c_i \log \hat{x}_i,$$
 (11)

$$\hat{x}_i = \frac{\exp(x_i)}{\sum_j \exp(x_j)},\tag{12}$$

where $c_i \in \{0,1\}$ is an indicator denoting whether the image contains the *i*-th category document and N_{cls} is the number of the total document categories.

Finally, we define the total loss as the weighted sum of the regression loss L_{Reg} , the classification loss L_{Cls} and the Line Loss L_{Line} :

$$L(x,c,p,g) = L_{Reg}(p,g) + \delta L_{Cls}(x,c) + L_{line}(p).$$
 (13)

where the weights δ , β and γ are chosen depending on the experimental results, and the values normally range from 0 to 1.

IV. EXPERIMENTAL EVALUATION

In this section, we demonstrate the configurations of the experiment at first, then we present the results observed. For the comparison experiment, we use the dataset from 'ICDAR 2015 SmartDoc Challenge 1' [3]. Training and inference setting details are listed in this section. The experimental results are compared to the previous work to show the advantages of our approach. Then we use the ablation study to analyze the contribution of each component of our work. Finally, we test our model on the MIDV-2019 dataset [25] to highlight the characteristic of our model, the ability to predict occluded corner points.

To evaluate the performance of our networks, we use the Jaccard Index (JI) measure [26] described in the ICDAR 2015 SmartDoc Challenge 1. First we remove the perspective transform of the ground-truth G and the predicted results S, then obtain the corrected quadrilaterals S' and S'. For each frame S', the JI is computed as:

$$JI(f) = area(G^{'} \cap S^{'})/area(G^{'} \cup S^{'}). \tag{14}$$

A. Training Details

Unless specified, we use MobilenetV2 with the width multiplier α equal to 0.35 (used to control the width of the network) as our backbone network. We set the number of regression points (N) to 100. Our network is trained with RMSprop optimizer, which uses only one set of hyperparameters (rho is set to 0.9, momentum is set to 0, and epsilon is set to 1e-7). We trained our networks for 1000 epochs, with an initial learning rate of 0.001 and a batch size of 128 images. The learning rate is reduced in a piecewise constant decay way, and is set as 0.0001, 0.00005, 0.00001 at the 250th, 700th and 850 epochs, respectively. Our backbone network weights are initialized with the weights pretrained on ImageNet [27]. We use the Xavier initializer [28] as the final dense layer. The input images are resized to which both the width and the height

are 224 pixels. Regarding the Line Loss function parameters, δ is set to 0.32, β and γ are configured as 0.0032.

B. Inference Details

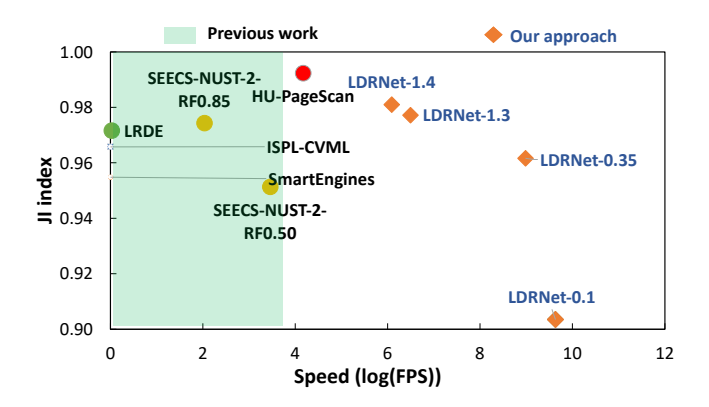
At first, we forward the input image through the network to obtain the quadrilateral points' coordinates of the documents and the predicted class. Then we multiply the quadrilateral points' coordinates by the width (W) and height (H) of the input image. Note that we only use four quadrilateral points' coordinates instead of the predicted N coordinates, because we found little difference between their performance. Thus we can remove the weights of the final dense layer that are not used for the four quadrilateral coordinates. The size of the input image is the same as we used for training. Our model is tested on iPhone11 using TNN [29] engine and can achieve 0.9849 JI while latency stays around 15.02ms.

C. Comparison of Jaccard Index

As shown in Table I, the images in the dataset can be divided into five categories according to different backgrounds. Only backgound05 is complex, with strong occlusions. We compare the performance of our method to 10 previous works. For each document, our LDRNet predicts 100 points and outperforms the previous works in terms of background02 and background05. For other backgrounds, LDRNet reaches comparable performance with the best ones. The overall JI of LDRNet exceeds the other methods except for HU-PageScan in [30], which does not provide the results of background01 to background05. However, HU-PageScan uses 8,873,889 trainable parameters which is over 21 times the number of parameters in our LDRNet-0.35 (denotes LDRNet with $\alpha = 0.35$). Therefore HU-PageScan requires significant memory and computing time thus can not fulfill the real-time demand on IDV frontend. Additionally, since HU-PageScan is segmentation-based, it only predicts the contour of the document. Thus postprocessing to determine the orientation and type of the document, which are essential for the subsequent verification process.

D. Comparison of Model Latency

Our Network is tested on iPhone11 using TNN engine. HU-PageScan is tested on a PC equipped with Intel Core i7 8700 processor, 8GB RAM, and 6GB NVIDIA GTX 1060 [30]. As depicted in Fig. 5, we have five settings of LDRNet, all using MobilenetV2 but with different values of α (0.1, 0.35, 0.75, 1.3, 1.4). Comparing the results from different settings of LDRNets, we observe that higher α leads to higher quantitative results but lower latency. We can observe that the JI of HU-PageScan is 0.0074 higher than LDRNet-1.4, whereas the speed is about 4x slower. It should be noted that our LDRNet model is tested on a mobile device. Our speed-prioritized model, LDRNet-0.1 runs 47x faster than HU-PageScan. LDRNet runs at the FPS ranging from 67 to 790 which meets the demand for localizing documents in the image frames in a live video (usually photographed at 30 FPS). For general usage, when precision is prioritized over latency,



Network	JI	Latency
LDRNet-1.4	0.9849	15.02 ms
LDRNet-1.3	0.9815	11.20 ms
LDRNet-0.75	0.9789	5.22 ms
LDRNet-0.35	0.9776	1.98 ms
LDRNet-0.1	0.9287	1.26 ms
HU-PageScan	0.9923	58.8 ms
SN2-RF0.85	0.9743	320 ms
SN2-RF0.50	0.9513	100 ms
LRDE	0.9716	>1 min

Fig. 5: The performance comparison between LDRNet and the previous document localization methods on the 'ICDAR 2015 SmartDoc Challenge 1' dataset. Our LDRNet tests are all configured with 100 points regression adding the Line Loss.

LDRNet-1.4 is the best option. Compared with LDRNet-1.4, LDRNet-0.35 has comparable precision, in addition, it is 7.6x faster and its model size is about 1MB, which is 10x smaller. Thus LDRNet-0.35 is more suitable for computation resources and storage resources limited devices.

E. Efficiency of Feature Fusion Module

To select the proper downsample and fusion operation, we run experiments configured with different feature fusion methods, as listed in Table II. The model in experiment 5 contains more parameters for convolution operations.

Based on the experimental results, we select the configuration in experiment 2 for the remainder of this paper, since its JI outperforms the other four.

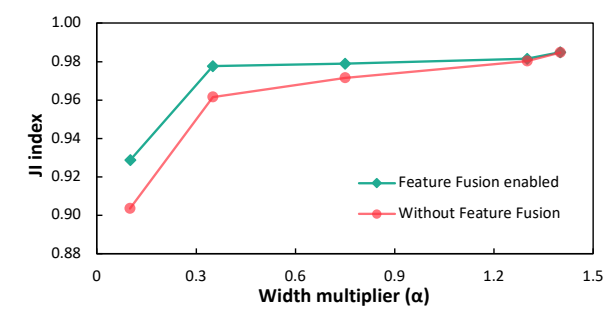


Fig. 6: The JI of LDRNet with different α and with or without feature fusion module. The number of regression points is set to 100. All are trained with Line Loss.

TABLE I: Performance compared with previous works. The metric is Jaccard Index measure.

Method	Background				Overall	
	01	02	03	04	05	
A2iA-1 [3]	0.9724	0.8006	0.9117	0.6352	0.1890	0.7788
A2iA-2 [3]	0.9597	0.8063	0.9118	0.8264	0.1892	0.8090
ISPL-CVML [3]	0.9870	0.9652	0.9846	0.9766	0.8555	0.9658
LRDE [3]	0.9869	0.9775	0.9889	0.9837	0.8613	0.9716
NetEase [3]	0.9624	0.9552	0.9621	0.9511	0.2218	0.8820
SEECS-NUST [3]	0.8875	0.8264	0.7832	0.7811	0.0113	0.7393
RPPDI-UPE [3]	0.8274	0.9104	0.9697	0.3649	0.2163	0.7408
SmartEngines [3]	0.9885	0.9833	0.9897	0.9785	0.6884	0.9548
SEECS-NUST-2 [14]	0.9832	0.9724	0.9830	0.9695	0.9478	0.9743
HU-PageScan [30]	/	/	/	/	/	0.9923
LDRNet (ours)	0.9877	0.9838	0.9862	0.9802	0.9858	0.9849

TABLE II: Different kinds of feature fusion models.

#	Downsample	Fusion	More parameters
1	average pooling	concatenate	×
2	average pooling	add	×
3	max pooling	concatenate	×
4	max pooling	add	×
5	convolution	add&convolution	\checkmark

Referring to the configuration of experiment 2 in Table II, we construct the feature fusion module using average pooling and add operation. To evaluate the efficiency of this feature fusion module, we run experiments with this module enabled and disabled. Fig. 6 compares the JI of these two scenarios with α ranging from 0.1 to 1.4. We can observe that the feature fusion-enabled models outperform those without feature fusion. Since the model complexity grows as we increase α , it is observed that the efficiency of our feature fusion module drops as the model becomes more complex. Thus in the cases that $\alpha > 1.0$, feature fusion is not recommended. For the models with $\alpha = 0.35$, the proposed feature fusion module significantly improves prediction accuracy.

F. Ablation Study

TABLE III: The JI and the sizes of parameters of LDRNet, using MobileNetV2-0.35 as backbone network (N refers to the number of points).

N	Line Loss	JI	Parameters
100		0.9776	670,251
36	V	0.9674	506,283
12		0.9540	444,795
36	V	0.9571	506,283
4	×	0.9435	424,299

As depicted in Table III, without the Line Loss, increasing the number of points from 4 to 36 can boost the JI from 0.9435 to 0.9571. When the Line Loss is applied, raising the number of points from 12 to 100 boosts the JI from 0.9540 to 0.9776. With the same number of points as 36, the introduction of the similarity loss and the distance loss improves the JI from 0.9571 to 0.9674. For regression loss, we have tried L2 loss

(MSE), L1 loss and log L1 loss. The performance of the L2 loss outperforms the other two in most experiments. The sizes of parameters during inference are equivalent (424,299) to the parameters irrelevant to the quadrilateral corner points that are removed.

TABLE IV: The JI, sizes of parameters during inference and model latency of LDRNet using MobilenetV2 with different α . The number of regression points is set to 100.

Alpha	Line Loss	JI	Parameters	Latency (ms)
1.4		0.9849	4,383,435	15.02
1.3	V	0.9815	3,784,363	11.20
0.75		0.9789	1,396,155	5.22
0.35	V	0.9776	424,299	1.98
0.35	×	0.9643	424,299	1.98
0.1	$\sqrt{}$	0.9287	107,403	1.26
0.1	×	0.9013	107,403	1.26



Fig. 7: Examples of occluded points prediction.

The backbone model size is the only variable that influences the model latency during inference. As observed from Table IV, when Line Loss is applied, reducing α from 1.4 to 0.1 causes the JI to drop from 0.9849 to 0.9287. Without the Line Loss, reducing α from 0.35 to 0.1 impairs the JI more severely, from 0.9643 to 0.9013. This indicates that the Line Loss can improve the precision of the LDRNet. As for α , 1.4 is sufficient for almost all the common situations. When the computation and storage resources are limited, setting α as 0.35 is suggested.

G. Predictions of the occluded Points

Benefiting from the task analysis and the network architecture, LDRNet is able to predict the occluded points, including the points occluded by other objects and the points out of the input image. This characteristic is crucial for the proposed edge intelligence-assisted IDV system since the identity document is usually occluded by the user's fingers during the interaction. For evaluation we test our model on the MIDV-2019 dataset, which contains video clips of identity documents captured by smartphones in low light conditions and with higher projective distortions [25]. There are 50 types of identity documents in the MIDV-2019 dataset, including 17 ID cards, 14 passports, 13 driving licenses and 6 other identity documents from different countries. Each identity document was captured under two different environments by two mobile devices separately, thus there are 200 video clips in total. For the model configurations, we use exactly the same as LDRNet-1.4 in the experiment on ICDAR-2015 dataset. The results show that LDRNet-1.4 can achieve the JI of 0.9617 on the MIDV-2019 dataset. The performance is slightly lower since the MIDV-2019 dataset is more complicated than the ICDAR-2015 dataset, due to the complex environments. The model latency remains stable as listed in Table IV.

The examples listed in Fig. 7 depict LDRNet's ability to predict the location of occluded points. Each case contains three images, namely, the input image (top left), the predicted corners on the input image (top right), the localized document after removing the perspective transformation (bottom). As depicted in Fig. 7(b), LDRNet can predict the corner occluded by fingers. In Fig. 7(c), a small part of the passport is out of the image, LDRNet predicts the location of the two occluded corners precisely. Even if more than half of the passport is out of the image, as illustrated in Fig. 7(d), our LDRNet predicts the occluded corners correctly. After removing the perspective transformation, we find that the passport is localized correctly.

V. CONCLUSION AND FUTURE WORK

In this paper, we present an Edge Intelligence-assisted Identity Document Verification framework to help banks and companies verify their customers' identities with high efficiency. A real-time document localization model, LDRNet, is proposed to address the performance challenge of IDV on mobile devices. LDRNet extracts the image features using neural networks and predicts the coordinates of quadrilateral points directly. We propose the novel loss function, Line Loss, and design the equal-division points feature to guarantee its efficiency and accuracy. On the backend, LDRNet reduces the response time of the general IDV process from 6 seconds to about 1.5 seconds, which greatly improves the user experience. Currently, LDRNet is being deployed in the IDV system of a company that serves about 3.8 million customers. Furthermore, LDRNet can be applied for other document localization cases. The experimental results show that LDRNet works up to 47x faster than other methods, while achieving comparable average JI. In future work, we will finetune the hyper-parameters more precisely, use low-level and high-level image features fusions like FPN, or a larger backbone, etc.

REFERENCES

- [1] S. Tang, C. Wang, J. Nie, N. Kumar, Y. Zhang, Z. Xiong, and A. Barnawi, "EDL-COVID: Ensemble deep learning for covid-19 case detection from chest x-ray images," *IEEE Transactions on Industrial Informatics*, vol. 17, no. 9, pp. 6539–6549, 2021.
- [2] Z. Zhou, X. Chen, E. Li, L. Zeng, K. Luo, and J. Zhang, "Edge intelligence: Paving the last mile of artificial intelligence with edge computing," *Proceedings of the IEEE*, vol. 107, no. 8, pp. 1738–1762, 2019.
- [3] J.-C. Burie, J. Chazalon, M. Coustaty, S. Eskenazi, M. M. Luqman, M. Mehri, N. Nayef, J.-M. Ogier, S. Prum, and M. Rusiñol, "Icdar2015 competition on smartphone document capture and ocr (smartdoc)," in 2015 13th International Conference on Document Analysis and Recognition (ICDAR). IEEE, 2015, pp. 1161–1165.
- [4] M. Sandler, A. Howard, M. Zhu, A. Zhmoginov, and L.-C. Chen, "Mobilenetv2: Inverted residuals and linear bottlenecks," in *Proceedings* of the IEEE conference on computer vision and pattern recognition, 2018, pp. 4510–4520.
- [5] K. Muhammad, S. Khan, V. Palade, I. Mehmood, and V. H. C. De Albuquerque, "Edge intelligence-assisted smoke detection in foggy surveillance environments," *IEEE Transactions on Industrial Informat*ics, vol. 16, no. 2, pp. 1067–1075, 2019.
- [6] O. Ronneberger, P. Fischer, and T. Brox, "U-net: Convolutional networks for biomedical image segmentation," in *International Conference on Medical image computing and computer-assisted intervention*. Springer, 2015, pp. 234–241.
- [7] P. Soille, Morphological image analysis: principles and applications. Springer Science & Business Media, 2013.
- [8] X.-C. Yin, J. Sun, S. Naoi et al., "Perspective rectification for mobile phone camera-based documents using a hybrid approach to vanishing point detection," in *International Workshop on Camera-Based Document Analysis and Recognition*, vol. 2, 2007, pp. 37–44.
- [9] X.-C. Yin, J. Sun, S. Naoi, K. Fujimoto, Y. Fujii, K. Kurokawa, and H. Takebe, "A multi-stage strategy to perspective rectification for mobile phone camera-based document images," in *Ninth International Conference on Document Analysis and Recognition (ICDAR 2007)*, vol. 2. IEEE, 2007, pp. 574–578.
- [10] R. G. Von Gioi, J. Jakubowicz, J.-M. Morel, and G. Randall, "Lsd: A fast line segment detector with a false detection control," *IEEE transactions* on pattern analysis and machine intelligence, vol. 32, no. 4, pp. 722– 732, 2008.
- [11] E. Carlinet and T. Géraud, "Mtos: A tree of shapes for multivariate images," *IEEE Transactions on Image Processing*, vol. 24, no. 12, pp. 5330–5342, 2015.
- [12] G. Lazzara, T. Géraud, and R. Levillain, "Planting, growing, and pruning trees: Connected filters applied to document image analysis," in 2014 11th IAPR International Workshop on Document Analysis Systems. IEEE, 2014, pp. 36–40.
- [13] Z. Tian, T. He, C. Shen, and Y. Yan, "Decoders matter for semantic segmentation: Data-dependent decoding enables flexible feature aggregation," in *Proceedings of the IEEE/CVF Conference on Computer* Vision and Pattern Recognition, 2019, pp. 3126–3135.
- [14] K. Javed and F. Shafait, "Real-time document localization in natural images by recursive application of a cnn," in 2017 14th IAPR International Conference on Document Analysis and Recognition (ICDAR), vol. 1. IEEE, 2017, pp. 105–110.
- [15] Y. Chen, C. Shen, X.-S. Wei, L. Liu, and J. Yang, "Adversarial posenet: A structure-aware convolutional network for human pose estimation," in Proceedings of the IEEE International Conference on Computer Vision, 2017, pp. 1212–1221.
- [16] K. B. Bulatov, "A method to reduce errors of string recognition based on combination of several recognition results with per-character alternatives," *Bulletin of the South Ural State University. Series: Mathematical Modeling and Programming*, vol. 12, no. 3, 2019.
- [17] L.-C. Chen, G. Papandreou, I. Kokkinos, K. Murphy, and A. L. Yuille, "Deeplab: Semantic image segmentation with deep convolutional nets, atrous convolution, and fully connected crfs," *IEEE transactions on* pattern analysis and machine intelligence, vol. 40, no. 4, pp. 834–848, 2017.

- [18] J. Long, E. Shelhamer, and T. Darrell, "Fully convolutional networks for semantic segmentation," in *Proceedings of the IEEE conference on computer vision and pattern recognition*, 2015, pp. 3431–3440.
- [19] G. Papandreou, T. Zhu, N. Kanazawa, A. Toshev, J. Tompson, C. Bregler, and K. Murphy, "Towards accurate multi-person pose estimation in the wild," in *Proceedings of the IEEE Conference on Computer Vision and Pattern Recognition*, 2017, pp. 4903–4911.
- [20] A. Bulat, J. Kossaifi, G. Tzimiropoulos, and M. Pantic, "Toward fast and accurate human pose estimation via soft-gated skip connections," in 2020 15th IEEE International Conference on Automatic Face and Gesture Recognition (FG 2020), 2020, pp. 8–15.
- [21] D. Tran, L. Bourdev, R. Fergus, L. Torresani, and M. Paluri, "Learning spatiotemporal features with 3d convolutional networks," in *Proceedings* of the IEEE international conference on computer vision, 2015, pp. 4489–4497.
- [22] L. Wang, Y. Xiong, Z. Wang, Y. Qiao, D. Lin, X. Tang, and L. Van Gool, "Temporal segment networks for action recognition in videos," *IEEE transactions on pattern analysis and machine intelligence*, vol. 41, no. 11, pp. 2740–2755, 2018.
- [23] T.-Y. Lin, P. Dollár, R. Girshick, K. He, B. Hariharan, and S. Belongie, "Feature pyramid networks for object detection," in *Proceedings of the IEEE conference on computer vision and pattern recognition*, 2017, pp. 2117–2125.
- [24] B. Hariharan, P. Arbeláez, R. Girshick, and J. Malik, "Hypercolumns for object segmentation and fine-grained localization," in *Proceedings of* the IEEE conference on computer vision and pattern recognition, 2015, pp. 447–456.
- [25] K. Bulatov, D. Matalov, and V. V. Arlazarov, "Midv-2019: challenges of the modern mobile-based document ocr," in *Twelfth International Conference on Machine Vision (ICMV 2019)*, vol. 11433. International Society for Optics and Photonics, 2020, p. 114332N.
- [26] W. Yue, Z. Wang, B. Tian, M. Pook, and X. Liu, "A hybrid model-and memory-based collaborative filtering algorithm for baseline data prediction of friedreich's ataxia patients," *IEEE Transactions on Industrial Informatics*, vol. 17, no. 2, pp. 1428–1437, 2020.
- [27] J. Deng, W. Dong, R. Socher, L.-J. Li, K. Li, and L. Fei-Fei, "Imagenet: A large-scale hierarchical image database," in 2009 IEEE conference on computer vision and pattern recognition. IEEE, 2009, pp. 248–255.
- [28] X. Glorot and Y. Bengio, "Understanding the difficulty of training deep feedforward neural networks," in *Proceedings of the thirteenth* international conference on artificial intelligence and statistics. JMLR Workshop and Conference Proceedings, 2010, pp. 249–256.
- [29] I. Lütkebohle, "TNN Github," https://github.com/Tencent/TNN, 2021, [Online; accessed 2-Feb-2021].
- [30] R. B. das Neves Junior, E. Lima, B. L. Bezerra, C. Zanchettin, and A. H. Toselli, "Hu-pagescan: a fully convolutional neural network for document page crop," *IET Image Processing*, vol. 14, no. 15, pp. 3890– 3898, 2020.